A Nanoelectronic Device Based on Endofullerene Peapod: Model Schematics and Molecular Dynamics Study

Jeong Won Kang*, Ki Ryang Byun*, Jun Ha Lee**, Hoong Joo Lee**, Ho Jung Hwang*

*School of Electrical and Electronic Engineering, Chung-Ang University
221-1 HukSuk-Dong, DongJak-Ku, Seoul 156-756, Korea, gardenriver@korea.com
** Department of Computer System Engineering, Sangmyung University
ChungNam 330-720, Korea

ABSTRACT

We investigated a nanoelectronic device based on multi *endo*-fullerenes shuttle memory element based on nanopeapods using classical molecular dynamics simulations. We suggested the model schematics of *endo*-fullerene shuttle memory device fabrication. The *endo*-fullerene shuttle memory element could operate a nonvolatile nano memory device. The switching speed, the applied force field, and the active region should be considered to design the *endo*-fullerene shuttle memory element.

Keywords: nanopepod memory device, bucky shuttle memory device, nano nonvolatile memory, endo-fullerene, molecular dynamics simulation

1 INTRODUCTION

The nanospaces inside nanocapsules or nanotubes have opened various applications as storage materials with high capacity and stability. In particular, self-assembled hybrid structures called "carbon nanopeapods" have been reported [1-3]. Recently, "boron-nitride nanopeapods" were also synthesized [4]. The application of nanopeapods ranges from nanometer-sized containers of chemical reactant to data storage [5,6]. Kwon *et al* [5] investigated 'bucky shuttle' memory device, which acted as nanometer-sized memory element, using molecular dynamics (MD) simulations. A lot of *endo*-fullerenes and *endo*-fullerene-encapsulated carbon nanotubes (CNTs) have been synthesized and investigated by experimental and theoretical methods [7-11]. Several field-effect molecule-shuttle memory elements based on nanopeapods have been investigated using classical MD simulations in our previous works [12-17].

While aligned bucky shuttle structures are difficult to be in self-assembly, nanopeapods can be synthesized in the aligned structures using bundles of single-walled nanotubes. If some processes, such as *endo*-fullerenes intercalation control, nanolithography, nanotube etching or cutting, nanotube capping or metal fillings for electrodes, are treated appropriately to the aligned nanotubes, the aligned bucky shuttles can be synthesized. Hence molecule-shuttle memory devices based on nanopeapods have been expected to bee realized by nanoscience and nanotechnology. This paper, using classical MD simulations, shows model schematics and probability of the molecule-shuttle electronic devices based on *endo*-fullerene nanopeapods.

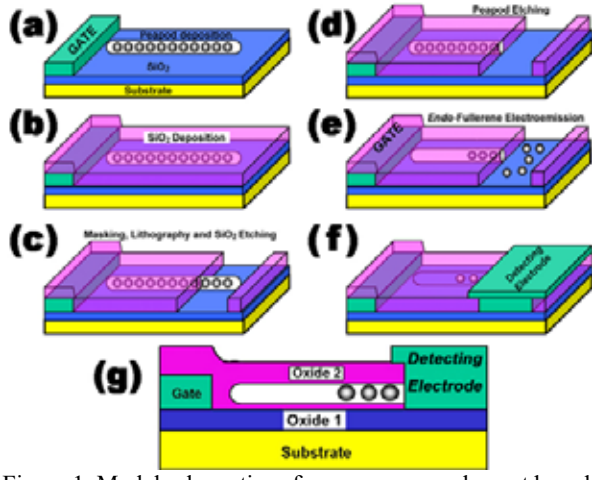

Figure 1. Model schematics of nano-memory-element based on nanopeapod. (a) The gate electrode is fabricated on the substrate covered with SiO_2 thin film; then nanopeapods are deposited on the SiO_2 thin film. (b) SiO_2 film growth on the surface. (c) A part of the nanopeapod is exposed by the SiO_2 removal process. (d) The exposed region of the nanopeapod is removed by the carbon etching processes. (e) Using the *endo*-fullerene electroemission process, some *endo*-fullerenes are emitted from the nanopeapod under the gate bias. (f) The electrode to detect the current impulse is deposited in the etched SiO_2 region. (g) The cut side view of the final structure.

2 MODEL SCHEMATICS

Figure 1 shows the model schematics of *endo*-fullerene shuttle memory device fabrication. The gate electrode is fabricated on the substrate covered with SiO_2 thin film; then nanopeapods are deposited on the SiO_2 thin film shown in Fig. 1(a). After the nanopeapod deposition, as Fig. 1(b) shows, SiO_2 film is grown on the structure of Fig. 1(a). On the opposite side of the nanopeapod for the gate electrode along the tube axis, the SiO_2 etching process is achieved

after masking and lithograph processes; then a part of the nanopeapod is exposed by the SiO_2 removal process shown in Fig. 1(c). The exposed region of the nanopeapod is removed by the nanotube etching processes; then, the structure shown in Fig. 1(d) is achieved. At this process, the edge of the nanotube should be opened to achieve the *endo*-fullerene electroemission from the nanotube. When the nanotube is fully filled with the *endo*-fullerenes, the *endo*-fullerene electroemission from the nanotube should be achieved for *endo*-fullerenes to migrate in the nanotube. Using the *endo*-fullerene electroemission process, some *endo*-fullerenes are emitted from the nanopeapod under the gate bias shown in Fig. 1(e). After the *endo*-fullerene electroemission process, the electrode to detect the current impulse is deposited in the etched SiO_2 region shown in Fig. 1(f). Figure 1(g) shows the cut side view of the final structure of Fig. 1(f). Since fully ionized *endo*-fullerene can be accelerated under external force fields, the *endo*-fullerene can be shuttled by the alternative external force fields. When the bits of the molecular-shuttle memory elements are defined by the positions of the *endo*-fullerenes, the data writing/erasing can be achieved from the gate bias. The positions of the *endo*-fullerenes can be controlled by the gate bias whereas the bit as the stored data can be detected by the current pulse of the detecting electrode as suggested by Kwon *et al*. [5].

3 INTERATOMIC POTENTIALS

3.1 Charge of endo-fullerene in nanotube

A lot of *endo*-fullerene peapods have been investigated in experimental and theoretical studies. In this work, we assume that the charge of the *endo* metal encapsulated in fullerene is fully ionized such as F^-, Ne, Na^+, K^+, Mg^{2+}, and Al^{3+} [18]. In order to move the encapsulated *endo*-fullerenes, the *endo*-fullerenes should carry a net charge. As the number of carbon atoms composed of fullerenes increases, the electron affinity generally increases [19]. The electron affinities of the *endo*-fullerenes are generally higher than those of the empty fullerenes [20-23]. Some *ab initio* calculations for the *endo*-fullerene peapods have shown the charge transfer from nanotubes to *endo*-fullerenes or fullerenes [24-26]. Chen and Lue [27] showed that the electron affinities of the CNTs were 1.0 ~ 1.5 eV by the theoretical fitting based on field emission experiments of CNTs. The above results imply that the charge of the encapsulated *endo*-fullerene is negative due to the charge transfer from nanotubes to *endo*-fullerenes. However, contrary results for the charge transfer have been reported. Cioslowski *et al*. [28] showed that the electron affinities of nanotubes with a finite length were generally higher than those of empty fullerenes. Kazaoui *et al*. [29] estimated that the average electron affinity of semiconductor single-wall CNTs was 4.8 eV by *in situ* measurements of optical absorption spectra. Hirahara *et al.* [30] discussed the possibility of the charge transfer from $Gd@C_{82}$ *endo*-fullerenes to single-wall CNTs. These results imply that the charge of the encapsulated *endo*-fullerenes can be positive. Therefore, we think that the charge transfer of *endo*-fullerene peapods should be investigated in further studies. Although there are contrary results for the charge transfer, the *endo*-fullerenes can have either a negative or a positive net charge. In this work, we follow the assumption by Kwon *et al.* [5] for the charge of the *endo*-fullerenes encapsulated in CNTs. In $K@C_{60}$ *endo*-fullerenes, which are known to form spontaneously under synthesis conditions in the presence of potassium, the valence electron of the encapsulated potassium atom is completely transferred to the C_{60} shell, and then $K^+@C_{60}^-$ is formed [31-34]. Kwon *et al.* assumed that the C_{60} shell is likely to transfer the extra electron to the graphitic outer capsule. The extra electron on the outer capsule will likely be further transferred to the structure that holds the bucky shuttle device. Therefore, Kwon *et al.* modeled the dynamics of the $K@C_{60}^+$ ion in the neutral carbon capsule by uniformly distributing a static charge of $+1e$ over the C_{60} shell. However, in our MD code, the *endo* metals were not included for computational efficiency, whereas the mass of C_{60} increased with the mass of the potassium atom and the charge of the C_{60} was assumed to be $+1e$ and was uniformly distributed on the C_{60}, such as in the previous study by Kwon *et al*. Therefore, the charge per carbon atom was assumed to be $+e/60$.

For C_{60} fullerene as a Faraday cage [35], when the applying electrostatic force field is 1 V/Å, the electrostatic force acting on K^+ is around 0.25 V/Å because of the field screening of the C_{60} fullerene. Therefore, the average electrostatic force field acting on carbon atom composed of the C_{60} fullerene will be 0.004 167 V/Å.

3.2 Interatomic potentials

For C-C interactions, we used the Tersoff-Brenner potential function that has been widely applied to C systems [36-38]. The long-range interactions were characterized with the Lennard-Jones 12-6 (LJ12-6) potential that was continually connected by the cubic spline functions with the Tersoff-Brenner potential such as methods by Mao *et al* [39] when the interatomic distance (r) is between 2.0 and 2.7 Å. The cutoff distance of the LJ12-6 with parameters $\varepsilon_C = 0.0024$ eV and $\sigma_C = 3.37$ Å was 10 Å. We assumed the Cu nanowires as the conductor material. For Cu–Cu and Cu–C, we used the Mores-type potential, a pair interatomic potential function, which have been widely used in many atomistic studies for nanoindentations and nanomechanics [40,41].

The MD simulations used the same MD methods as were used in our previous works [42,43]. The MD code used the velocity Verlet algorithm, and neighbor lists to improve computing performance. MD time step was 5×10^{-4} ps. A Gunsteren-Berendsen thermostat was used to control

temperature for all atoms except for fullerenes. The structure was initially relaxed by the steepest descent method; then the atoms of both edges were fixed during the MD simulations and on the other atoms, MD methods were applied.

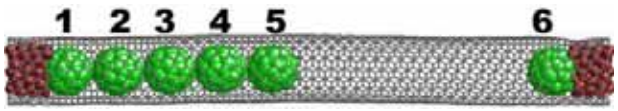

Figure 2. (a) The positions of the C_{60}^{+}s and (b) the total potential energy as a function of MD time when the external applying field is –0.2 V/Å.

4 RESULTS AND DISCUSSION

Figure 2 shows the initial structure for the MD simulations of the *endo*-fullerene shuttle in the nanotube. Six *endo*-fullerenes were encapsulated into a (10, 10) CNT with 117 Å length, and both Cu electrodes with 7 Å was obtained from our previous work [43] that shows the Cu nanowires encapsulated in the armchair CNT. The minimum potential energies were found near the both ends of the nanopeapod and the activation energy barrier was 0.399 eV [14]. Since the binding energy between a Cu electrode and a C_{60} was higher than that between C_{60}s, active elements became the structure as shown in Fig. 2 after alternative force fields were successively applied. Two *endo*-fullerenes labeled by 1 and 6 were always attached at the both end electrodes and the shuttle media were always the central four *endo*-fullerenes.

The position control of the *endo*-fullerenes by the electromigration processes is the basis of the bucky-shuttle memory device of Kwon *et al*. [5]. Figure 4 shows the total potential energy of the system (Fig. 3(a)) and the position variations of the shuttle fullerenes along the tube axis (Fig. 3(b)) as a function of MD time. The applied force field is shown in Fig. 3(c). External force field was initially 0.06 V/Å to 5 ps, increased to 0.12 V/Å by a exponential function to 6 ps, continually maintained 0.12 V/Å to 25 ps, and then decreased to 0.06 V/Å by an exponential function to 30 ps. The applied force fields were disappeared after 30 ps. Peaks in the total potential energies were found when the *endo*-fullerenes collided with the electrode or with each other.

Times required for entire bit flop were about 80 ps due to the rebound events of the *endo*-fullerenes, as shown in Fig. 3. Though the external force field vanished, the *endo*-fullerenes were safely settled at the expected bit flop. This means that the force fields for bit writing/erasing need not be applied during entire bit flop. Since the activation energy barrier of an *endo*-fullerene inside the (10, 10) CNT was 0.399 eV [14], the memory system based on *endo*-fullerene peapods can be applied to a nonvolatile nano memory element. When the magnitude and the duration of the external force fields are appropriately applied to this system, the rebound events during the bit flop can be reduced and the bit flop speed can be also upgraded. When the active region and the number of the *endo*-fullerenes are also properly selected, the rebounded events may be unimportant in the operation of this system. When the applied force fields were very low in the conditions that the *endo*-fullerenes can be switched, these rebounded events were not found. The switching speed was very low under the very low applied fields. When high external force fields were applied, the speeds of the *endo*-fullerenes were also high whereas the entire bit flops were achieved after a long time because of several rebounded events. Therefore, to design the system suggested in this work, the switching speed, the applied force field, and the active region should be considered.

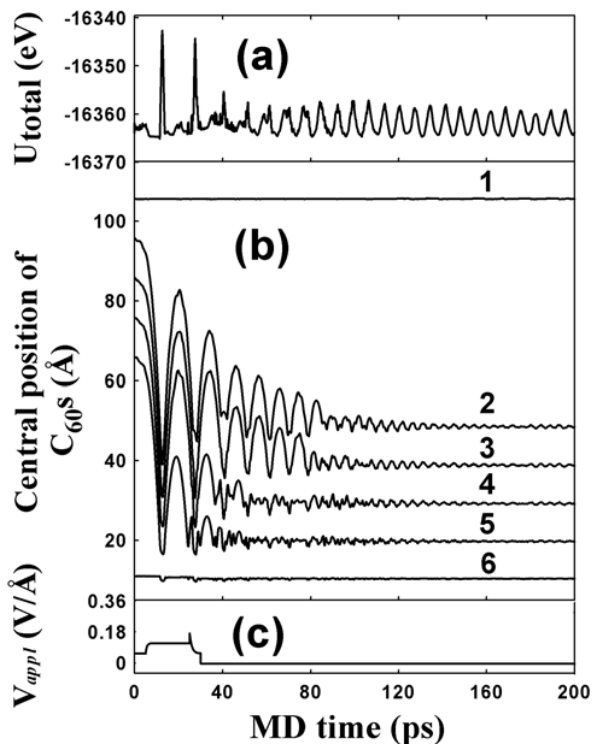

Figure 3. (a) Total potential energy of the system and (b) the position variations of the C_{60}^{+}s along the tube axis as functions of MD time and external force field.

5 SUMMARY

In summary, we studied the *endo*-fullerene shuttle memory element based on nanopeapods using classical molecular dynamics simulations. We suggested the model schematics of *endo*-fullerene shuttle memory device fabrication. The systems could operate nonvolatile nano memory devices when the positions of *endo*-fullerenes were controlled by gate bias. Our molecular dynamics simulations showed that the switching speed, the applied

force field, and the active region should be considered to design the nano device suggested in this work.

ACKNOWLEDGEMENTS

This research was supported by grant No. R01-2004-000-10864-0 from the Korea Science and Engineering Foundation.

REFERENCES

[1] B.W. Smith, M. Monthioux, D.E. Luzzi, Nature 396 (1998) 323.
[2] B. Burteaux, A. Claye, B.W. Smith, M. Monthioux, D.E. Luzzi, J.E. Fischer, Chem. Phys. Lett. 310 (1999) 21.
[3] B.W. Smith, M. Monthioux, D.E. Luzzi, Chem. Phys. Lett. 315 (1999) 31.
[4] W. Mickelson, S. Aloni, W.Q. Han, J. Cumings, A. Zettl, Science 300 (2003) 467.
[5] Y.K. Kwon, D. Tománek, S. Iijima, Phys. Rev. Lett. 82 (1999) 1470.
[6] R.F. Service, Science 292 (2001) 45.
[7] J. Cioslowski, E.D. Fleischmann, J. Chem. Phys. 94 (1991) 3730.
[8] J. Sloan, S. Friedrichs, R.R. Meyer, A.I. Kirkland, J.L. Hutchison, M.L.H. Green, Inorganica Chimica Acta 330 (2002) 1.
[9] M. Monthioux, Carbon 40 (2002) 1809.
[10] D. Qian, G.J. Wagner, W.K. Liu, M-F. Yu, R.S. Ruoff, Appl. Mech. Rev. 55 (2002) 495.
[11] P.W. Chiu, G. Gu, G.T. Kim, G. Philipp, S. Roth, S.F. Yang, S. Yang, Appl. Phys. Lett. 23 (2001) 3845.
[12] J.W. Kang, H.J. Hwang, J. Phys. Soc. Japan. 73 (2004) 1077.
[13] J.W. Kang, H.J. Hwang, J. Korean Phys. Soc. 44 (2004) 879.
[14] W.Y. Choi, J.W. Kang, H.J. Hwang, Physica E 23 (2004) 135.
[15] J.W. Kang, H.J. Hwang, Carbon 14 (2004) 3018.
[16] J.W. Kang, H.J. Hwang, Jpn. J. Appl. Phys. 73 (2004) 4447.
[17] J.W. Kang, W.Y. Choi, H.J. Hwang, J. Comp. Theori. Nanosci. 1 (2004) 199.
[18] J. Cioslowski, E.D. Fleischmann, J. Chem. Phys. 94 (1991) 3730.
[19] O.V. Boltalina, E.V. Dashikova, L.N. Sidorov, Chem. Phys. Lett. 256 (1996) 253.
[20] M.-H. Du, H-P. Cheng, Phys. Rev. B 68 (2003) 113402.
[21] J. Lu, X. Zhang, Z. Zhao, Solid State Commu. 110 (1999) 565.
[22] I.N. Ioffe, A.S. Levlev, O.V. Boltalina, L.N. Sidorov, H.C. Dorn, S. Stevenson, G. Rice, Inter. J. Mass Spectrometry 213 (2002) 183.
[23] K. Kobayashi, Y. Sano, S. Nagase, J. Comp. Chem. 22 (2001) 1353.
[24] S. Okada, M. Otani, A. Oshiyama, Phys. Rev. B 67 (2003) 205411.
[25] S. Okada, S. Saito, A. Oshiyama, Phys. Rev. Lett. 86 (2001) 3835.
[26] Y. Cho, S. Han, G. Kim, H. Lee, J. Ihm, Phys. Rev. Lett. 90 (2003) 106402.
[27] S.-Y. Chen, J-T. Lue, Phys. Lett. A 309 (2003) 114.
[28] J. Cioslowski, N. Rao, D. Moncrieff, J. Am. Chem. Soc. 124 (2002) 8485.
[29] S. Kazaoui, N. Minami, N. Matsuda, H. Kataura, Y. Achiba, Appl. Phys. Lett. 78 (2001) 3433.
[30] K. Hirahara, K. Suenaga, S. Bandow, K. Kato, T. Okazaki, H. Shinohara, S. Iijima, Phys. Rev. Lett. 85 (2000) 5384.
[31] Y.S. Li, D. Tománek, Chem. Phys. Lett. 221 (1994) 453.
[32] G. Gao, T. Cagin, W.A. Goddard, Phys. Rev. Lett. 80 (1998) 5556.
[33] G. Chen, Y. Guo, N. Karasawa, W.A. Goddard, Phys. Rev. B 48 (1993) 13959.
[34] Y. Guo, N. Karsawa, W.A. Goddard, Nature 351 (1991) 464.
[35] P. Delaney, J.C. Greer, Appl. Phys. Lett. 84 (2004) 431.
[36] J. Tersoff, Phys. Rev. B 38 (1988) 9902.
[37] J. Tersoff, Phys. Rev. B 39 (1989) 5566.
[38] D.W. Brenner, Phys. Rev. B 42 (1990) 9458.
[39] Z. Mao, A. Garg, S.B. Sinnott, Nanotechnology 10 (1999) 273.
[40] T.H. Fang, C.I Weng, Nanotechnology 11 (2000) 148.
[41] L. Zhang, H. Tanaka, Wear 211 (1997) 44.
[42] J.W. Kang, H.J. Hwang, Nanotechnology 15 (2004) 614.
[43] W.Y. Choi, J.W. Kang, H.J. Hwang, Phys. Rev. B 68 (2003) 193405.